GRID WAYMARK BASEBAND UNDERWATER ACOUSTIC TRANSMISSION MODEL

Li Liao, Benjamin Henson, Yuriy Zakharov

Department of Electronic Engineering, University of York, UK
Email: ll924@york.ac.uk, bth502@york.ac.uk, yury.zakharov@york.ac.uk.

Abstract: *In this paper, we propose and investigate a model for signal transmission in fast-varying underwater acoustic (UWA) channels. In particular, this model can be used for numerical investigation of UWA communication systems with moving transmitter and/or receiver. Known modelling techniques suffer from high computational complexity for signal transmission sessions of high duration and are only applicable to single-input single-output communication systems. The known Waymark simulator can efficiently deal with long-duration transmission sessions. However, its running speed is limited by the ray tracing used for computing the waymark impulse responses. We propose to pre-compute ray parameters on a space (depth-range) grid, similarly to how it is done in the known VirTEX simulator, and use the ray parameters for the waymark impulse response computation, thus speeding up the simulation. Numerical examples show that this approach can reduce the simulator running time by 10-20 times compared to the baseband Waymark simulator, and, for some scenarios, make the simulation time close to the real time.*

Keywords: *Underwater acoustic communications, VirTEX, Waymark*

1. INTRODUCTION

The underwater channel is considered as one of the most difficult channels for communications [1]. The performance of underwater acoustic communication systems is heavily dependent on the propagation environment. Sea experiments are often used to assess the communication performance, but they are expensive and difficult to conduct. To reduce the cost, a simulation of the signal transmission can be used. It can guarantee similar conditions when comparing different systems and provide reliable monitoring of the environment and thus give a valuable interpretation of experimental results. Therefore,

it is highly desirable to have an efficient simulator for underwater acoustic signal transmission [2], [3]. There have been a number of approaches to deal with this problem, for example using a static channel impulse response [4] obtained from acoustic field computation [5], [6], or a model based on random fluctuations of complex amplitudes of eigenpaths. Some models introduce frequency shifts in eigenpaths and a statistical model for multipath amplitudes [7]. Some approaches use a measured time-varying channel response and random local displacements based on direct replay [8], [2].

The VirTEX (Virtual Timeseries Experiment) simulator [9] operates by post processing the outputs produced by the Bellhop ray tracing program [10]. This simulator performs the ray tracing on a grid within a depth-range frame of interest. The ray parameters on the grid points are then used for approximation of the acoustic field in the frame. The VirTEX can simulate the transmission of relatively short signals between moving transmitter and receiver, and it requires computation of the channel impulse response from the acoustic field computations at every signal sample, which is complicated when dealing with signals at a high carrier frequency.

Another promising approach in the virtual signal transmission [9], [11] is the Waymark simulator [12], also allowing modelling the signal transmission for moving transmitter and receivers. The motion-induced channel time variations are modelled by sampling the transmitter/receiver trajectory at a rate much lower than the signal sampling rate and calculating, for each waymark position, the channel impulse response from the acoustic-field computation. The Waymark impulse responses are then used for interpolation of the time-varying channel impulse response at a sampling rate chosen with respect to the highest frequency in the spectrum of the transmitted signal. The high sampling frequency may result in a high running time for the original Waymark simulator.

A further development of the Waymark model [12] with the aim to significantly reduce the simulation time is based on baseband processing [13]. However, the efficiency of the baseband Waymark model is now limited by the ray tracing (the Bellhop program [10] in our case) used for computing the impulse responses at waymarks. In this paper, we propose to pre-compute the ray parameters on a space (depth-range) grid, similarly to how it is done in the VirTEX simulator [9], then save this grid map with arrival information at every grid point in memory. When in simulation, the ray parameters at every waymark are approximately computed by combining the pre-computed arrivals at four grid points around the waymark location rather than running Bellhop, thus speeding-up the computations.

2. UNDERWATER ACOUSTIC CHANNEL SIMULATOR

Waymark Model: In a time-varying channel, the noise-free signal at a receiver is described as a convolution [14]:

$$y(t) = \int_{-\infty}^{\infty} h(t,\tau)s(t-\tau)\mathrm{d}\tau, \quad t \in \left[0, T_{sig}\right] , \tag{1}$$

where $h(t,\tau)$ is the passband channel impulse response at time t, $s(t)$ is the transmitted signal and T_{sig} is the signal duration. At time t the channel impulse response can be represented as the sum of multipath components [15]:

$$h(t,\tau) = \sum_{p=1}^{L} A_p(t)\delta(\tau - \tau_p(t)), \tag{2}$$

where L is the number of arrivals, $A_p(t)$ is the time-varying amplitude of the p th path and $\tau_p(t)$ represents the corresponding delay. The time-varying delay $\tau_p(t)$ is defined by the path geometry, which encompass any movement in the system ultimately representing the Doppler effect.

In the Waymark model [12], a sequence of points (waymarks) is set along the receiver/transmitter trajectory, and the impulse response at every waymark is calculated using the arrivals computed by the Bellhop ray-tracing program [10]. The time interval in the trajectory between waymarks is typically much longer than the signal sampling interval due to the slow variation of the channel impulse response from one signal sample to another. This long waymark interval reduces the simulation time greatly when compared to ray-tracing for every signal sample interval.

To reduce the simulation time further, an extension to the Waymark model in [12] creates a time-varying channel model using the baseband equivalent representation of the signals and channel, which allows the processing on the signal propagating through the channel also to be at baseband frequencies [13]. The processing therefore is performed at a lower sampling rate depending on the signal bandwidth. In addition, this model has the ability to model longer channel impulse responses with the same resources, which helps to deal with more extreme underwater environments.

As described in [13], in the baseband Waymark model, the original signal spectrum is shifted to centre around zero and a low pass filter applied. The low pass filter chosen is the raised cosine filter [16]. The baseband equivalent transmitted signal $s_e(nT_s)$ can be approximated by:

$$s_e(nT_s) = \sum_{k=-K/2}^{K/2-1} [s(kT_s)e^{-j2\pi f_c kT_s}]r(nT_s - kT_s), \quad n = 0,..., N-1, \tag{3}$$

where the raised cosine impulse response [16] is given by:

$$r(nT_s) = \mathrm{sinc}(f_0 nT_s)\frac{\cos(\pi f_0 \alpha nT_s)}{1-(2f_0\alpha nT_s)^2}, \tag{4}$$

where T_s is the original sampling period of the passband signal, $N = T_{sig}/T_s$, K is the raised cosine filter length, α represents the roll-off factor, and f_0 is the upper bound of the baseband frequencies.

Once the transmitted signal has been transformed into the baseband equivalent $s_e(nT_s)$, the sampling interval T_s then can be increased to a longer sampling period T_d. The baseband signal at the receiver is then obtained via the baseband filtering:

$$y_e(n_d T_d) = \sum_{i=0}^{I-1} h_e(n_d T_d, iT_d)s_e(n_d T_d - iT_d), \quad n_d = 0,..., N_d - 1, \tag{5}$$

where $h_e(n_d T_d, iT_d)$ is the baseband channel impulse response at time $t = n_d T_d$, $N_d = T_{sig}/T_d$, I is the number of channel taps and i is the index of channel tap. The baseband channel impulse response $h_e(n_d T_d, iT_d)$ at every sample $n_d T_d$ is then computed by a spline approximation [12] using the baseband channel impulse responses $h_{e,m}(iT_d)$ calculated at waymark points. Once passed through the channel the output baseband signal $y_e(n_d T_d)$ is upsampled back to the original sampling frequency as $y_e(nT_s)$, and upshifted back to passband. Due to the relatively slow speed of sound, the channel delay variations are very important in the restoration of the signal to the passband. Therefore, the upshift of

the signal needs to take into account the delay that was applied to the input signal at each sample point. The upshifted post channel signal is then calculated as:

$$y(nT_s) = \Re\{y_e(nT_s)e^{j2\pi f_c(nT_s-\tau_n)}\}, \quad (6)$$

where $y(nT_s)$ is the output signal sample, $y_e(nT_s)$ is upsampled baseband output signal and τ_n represents the estimated additional delay at each output sample instant. The delay τ_n is computed using the spline interpolation between the waymark delays.

Grid Waymark Model: To speed up the computations in the Waymark model further, the Grid Waymark model is proposed. Similar to the VirTEX model in [9], we are using a regularly spaced grid to describe the volume of water that the signal propagates through. The model interpolation is performed on the amplitude and delay of arrivals of the multipath components. An interpolated point (waymark) between the grid points is gathering the weighted arrivals at the four surrounding grid points as shown in Fig. 1 and Fig. 2.

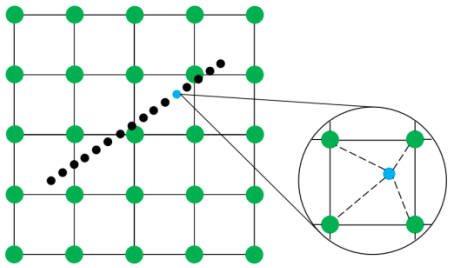

Fig.1: Receiver trajectory with waymarks (black, blue) in a grid field (green). The acoustic field at a waymark point is combined with the weighted arrivals at four grid points around it.

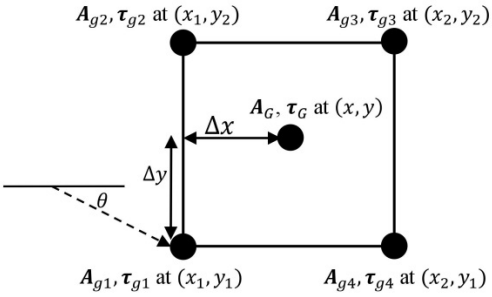

Fig.2: Four points of the grid for a ray tracing computation at a waymark. The arrivals are pre-computed at the four corners and any point in the interior is computed through interpolation of the weighted amplitudes and adjusted delays at grid points. A sample arrival is shown traveling at angle θ.

The attenuations from the four grid points are weighted and gathered to obtain complex amplitudes $\mathbf{A}_G$ at the waymark (trajectory) point (x, y), and the corresponding delays $\boldsymbol{\tau}_G$ are adjusted by the ray path travel time differences between the corners of the computational grid and the interpolated point (see [9] for more details). The arrival amplitudes at each of the grid points are weighted and combined as:

$$\mathbf{A}_G = \left[(1-w_x)(1-w_y)\mathbf{A}_{g1}^T \quad (1-w_x)w_y\mathbf{A}_{g2}^T \quad w_x w_y \mathbf{A}_{g3}^T \quad w_x(1-w_y)\mathbf{A}_{g4}^T\right]^T. \quad (7)$$

Here we assume that the maximum number of arrivals at each grid point is L, then $\mathbf{A}_{g1}$, $\mathbf{A}_{g2}$, $\mathbf{A}_{g3}$, and $\mathbf{A}_{g4}$ are column vectors of length L; they represent the arrival amplitudes at each of four grid points around the waymark point (x, y). The weights w_x and w_y are given by [9]: $w_x = (x-x_1)/(x_2-x_1)$ and $w_y = (y-y_1)/(y_2-y_1)$. Thus, w_x represents a proportional distance in the x direction and w_y represents a proportional distance in the y direction.

As shown in Fig. 2, the dashed line represents an arrival traveling at angle θ at the lower left grid point. The delay time for that arrival is adjusted from position (x_1, y_1) to

position (x, y) by the distance divided by the sound speed [9]. The adjusted delay is given by $\Delta_{delay} = (\Delta x \cos\theta + \Delta y \sin\theta)/c$, where $\Delta x = x - x_1$, $\Delta y = y - y_1$ for the grid point (x_1, y_1) in this example, and c is the sound speed at (x_1, y_1). The corresponding delays of arrival at (x, y) then are given by

$$\boldsymbol{\tau}_G = \left[\boldsymbol{\tau}_{g1}^T + \Delta_{\boldsymbol{\tau}1}^T \quad \boldsymbol{\tau}_{g2}^T + \Delta_{\boldsymbol{\tau}2}^T \quad \boldsymbol{\tau}_{g3}^T + \Delta_{\boldsymbol{\tau}3}^T \quad \boldsymbol{\tau}_{g4}^T + \Delta_{\boldsymbol{\tau}4}^T\right]^T, \tag{10}$$

where $\boldsymbol{\tau}_{g1}$, $\boldsymbol{\tau}_{g2}$, $\boldsymbol{\tau}_{g3}$ and $\boldsymbol{\tau}_{g4}$ are $L \times 1$ column vectors; they represent the delays of arrival at grid points corresponding to $\mathbf{A}_{g1}$, $\mathbf{A}_{g2}$, $\mathbf{A}_{g3}$, and $\mathbf{A}_{g4}$. Vectors $\Delta_{\boldsymbol{\tau}1}$, $\Delta_{\boldsymbol{\tau}2}$, $\Delta_{\boldsymbol{\tau}3}$ and $\Delta_{\boldsymbol{\tau}4}$ contain adjusted delays Δ_{delay} of all arrivals at (x_1, y_1), (x_1, y_2), (x_2, y_2), (x_2, y_1).

With the complex amplitudes of arrivals $\mathbf{A}_G$ and corresponding delays $\boldsymbol{\tau}_G$, which characterize the acoustic field, we can find the channel frequency response $H_e(\omega)$ at that waymark (x, y). The baseband channel impulse response $h_e(iT_d)$ is obtained from $H_e(\omega)$ by the inverse Fourier transform.

At waymark m, the channel frequency response $H_{e,m}(\omega_q)$ at a frequency ω_q is computed as:

$$H_{e,m}(\omega_q) = \sum_{l=1}^{M} C_l e^{-j\omega_q(\tau_{G,l} - \tau_{\min})}, \tag{11}$$

where M is the number of eigenpaths gathered for the waymark point, $\tau_{\min}$ is the minimum delay (the common propagation delay) for all the paths, which is removed from all arrivals to reduce the size of the impulse response at waymark point as described in [12]. C_l is the baseband complex amplitude of the lth arrival and $\tau_{G,l}$ is the corresponding delay. The complex amplitude of the multipath arrival at the baseband is given by [15]: $C_l = \mathbf{A}_{G,l} e^{-j2\pi f_c \tau_{G,l}}$, where $\mathbf{A}_{G,l}$ is the complex amplitude of the lth arrival gathered at waymark m, and f_c is the carrier frequency.

Assuming Q frequencies of interest ω_q, the impulse response $h_{e,m}(iT_s)$ is then obtained by the inverse Fourier transform:

$$h_{e,m}(iT_d) = \sum_{q=0}^{Q-1} H_{e,m}(\omega_q) e^{j\omega_q iT_d}. \tag{13}$$

The structure of the proposed simulator is shown in Fig. 3, as a development from the original system in [13]. In this development, the acoustic field at waymark m is computed by gathering the weighted arrivals at four grid points around the waymark point, rather than calling the Bellhop program. The channel frequency response $H_{e,m}(\omega_q)$ at waymark m and the impulse response $h_{e,m}(iT_d)$ are then computed from the frequency response. With the baseband equivalent representation, the processing is allowed to be at baseband frequencies and performed at a lower sampling rate, thus reducing the simulation time. The splitting of the channel into two components, the composite delay and impulse response, allows more accurate interpolation of the channel impulse response between waymarks. Since the variation of the channel impulse response from one signal sample to another is considered slow, the sampling interval is increased from T_s to $T_d = \eta \times T_s, (\eta >> 1)$, to give a lower sampling rate, and consequently reduces the computation. The local spline interpolation is then used for recovering the impulse response for all signal sampling instants. The local interpolation between waymarks

allows removing any constrains on the duration of the signal transmission simulation session.

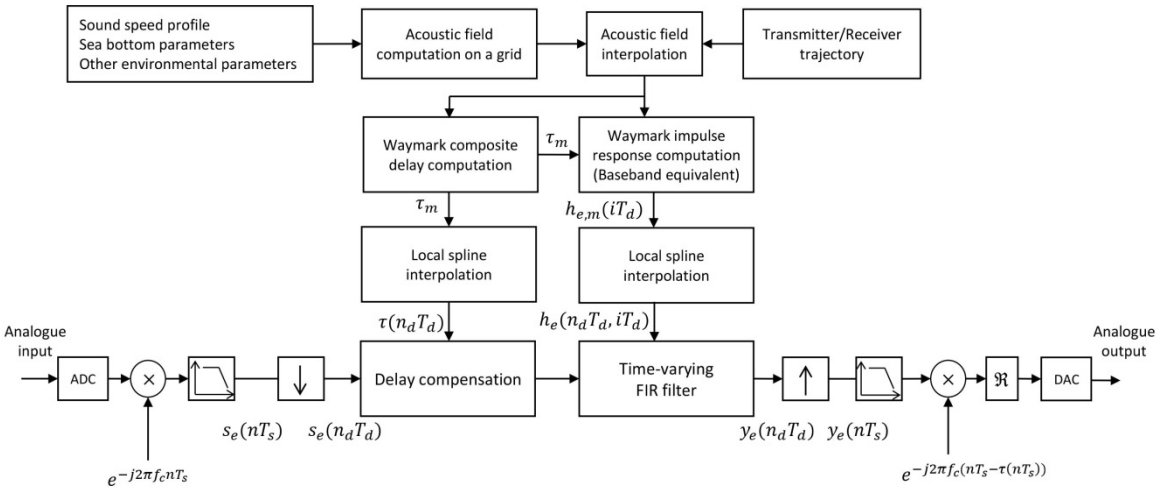

Fig. 3: A block diagram of the underwater acoustic channel simulator as a development on the system presented in [13].

3. SHALLOW WATER EXPERIMENTS

In this section, some examples are given to illustrate the proposed simulator and compare it with the original baseband Waymark and VirTEX models.

1) Simplified Environment Test: The simulation environment is as follows.

A 10 kHz tone signal is transmitted. It is sampled at a 40 kHz sample frequency. The signal duration is 100 seconds. The underwater environment is described by a flat Sound Speed Profile (SSP); the speed of sound is constant 1500 m/s from the bottom to surface. The sea bottom is flat at 200 meters depth and the surface is flat calm. Both the receiver and transmitter are at a depth of 100 meters. The range between them varies as 1000 m + $v_c t$ m, (v_c = 5 m/s). The decimation factor is 64, giving the signal sample interval T_d = 64 × T_s = 1.6 ms.

With a 10 kHz tone the motion was expected to result in a Doppler shift of around -33.3 Hz. The waymark interval was set to 0.0512 seconds. Fig. 4 shows the spectrum of the channel output from the original baseband Waymark, VirTEX and proposed Grid Waymark models. The peaks in the figure are due to multipath components with slightly different Doppler spreads.

The simulation was running in Matlab (version R2013a) under Windows 7 operating system with a 3.4 GHz Intel Core i7 CPU and 8 GB of RAM. For the original baseband Waymark model, simulating 120 seconds of transmission time requires 4662 seconds, this number is mostly due to the Bellhop ray-tracing called at every waymark. For the proposed Grid Waymark model with grid step of 0.25 m, the same as the waymark step in the original baseband Waymark model, this simulation only takes 226 seconds, which is almost a real time simulation. This is a significant reduction in computation compared to the original baseband Waymark model, it is about 20 times faster with the proposed Grid Waymark model.

2) Complex Environment Test: To compare these three models with a more complex environment, the 10 kHz tone is transmitted in the SWellEx-96 [17] SSP and a section of the trajectory from Event S5. The simulation environment is as follows.

A 10 kHz tone of 100s duration is transmitted, sampled at 40 kHz sampling frequency. The sea bottom is flat and the surface is flat calm. Locations of the transmitter and the receiver are from the SWellEx-96 event S5 localized data [18]. The transmitter was moving towards the receiver at 2.5 m/s. The decimation factor is 64.

Fig. 5 shows the spectrum of the channel output from the original baseband Waymark, VirTEX and the proposed Grid Waymark models. The waymark interval for the Waymark model [13] and the Grid Waymark model was 0.0512 seconds. The Doppler spreads around the main peaks are again generally agreed. For the Waymark model, 14009 seconds is required in this simulation, while the proposed Grid Waymark requires 1476 seconds, which shows about 10 times faster computation.

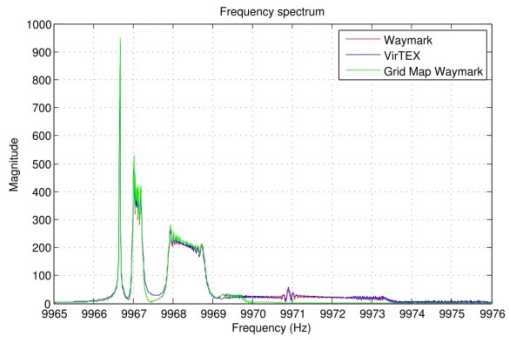

Fig. 4: The received signal spectrum from the Waymark, VirTEX and Grid Waymrk models with a flat SSP sound environment.

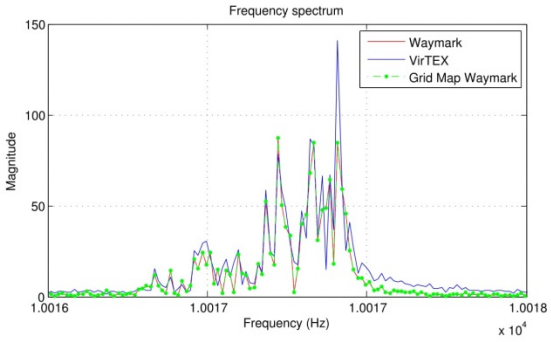

Fig. 5. The received signal spectrum from the Waymark, VirTEX and Grid Waymrk models with the SWellEx environment and trajectory.

4. CONCLUSION

In this paper, a further extension to the Waymark model proposed in [12] and [13] is described as the Grid Waymark model. This model combines the Waymark model with the VirTEX pre-computing the acoustic field on a space grid. It computes the waymark impulse responses by gathering weighted ray parameters from the grid points around the waymark. The Grid Waymark model has a significant advantage in computation speed compared to the original baseband Waymark model.

The original baseband Waymark, VirTEX and Grid Waymark have been compared. The results show similarity with the major features such as the Doppler shifts. The computation time taken with Grid Waymark model is significantly less than that with the original Waymark model.

REFERENCES

[1] **J. Preisig**, "Acoustic propagation considerations for underwater acoustic communications network development", *ACM SIGMOBILE Mobile Computing and Communications Review*, vol. 11, pp. 2-10, 2007.
[2] **M. Stojanovic and J. Preisig**, "Underwater acoustic communication channels: Propagation models and statistical characterization", *IEEE Communications Magazine*, vol. 47, no. 1, pp. 84–89, 2009.
[3] **I. F. Akyildiz, D. Pompili, and T. Melodia**, "Underwater acoustic sensor networks: research challenges", *Ad Hoc Networks*, vol. 3, no. 3, pp. 257–279, 2005.
[4] **D. B. Kilfoyle and A. B. Baggeroer**, "The state of the art in underwater acoustic telemetry", *IEEE Journal of Oceanic Engineering*, vol. 25, no. 1, pp. 4–27, 2000.
[5] **M. B. Porter**, "The KRAKEN normal mode program", DTIC Document, Tech. Rep., 1992.
[6] **M. B. Porter and H. P. Bucker**, "Gaussian beam tracing for computing ocean acoustic fields", *The Journal of the Acoustical Society of America*, vol. 82, no. 4, pp. 1349–1359, 1987.
[7] **X. Geng and A. Zielinski**, "An eigenpath underwater acoustic communication channel model", In *OCEANS'95. MTS/IEEE. Challenges of Our Changing Global Environment. Conference Proceedings*, San Diego, California, USA, Vol. 2, pp. 1189-1196, 1995.
[8] **R. Otnes, P. A. van Walree, and T. Jenserud**, "Validation of replay-based underwater acoustic communication channel simulation", *IEEE Journal of Oceanic Engineering*, vol. 38, no. 4, pp. 689–700, 2013.
[9] **M. Siderius and M. B. Porter**, "Modeling broadband ocean acoustic transmissions with time-varying sea surfaces", *The Journal of the Acoustical Society of America*, vol. 124, p. 137, 2008.
[10] **M. B. Porter**, "The BELLHOP manual and user's guide: Preliminary draft", Heat, Light, and Sound Research, Inc, Tech. Rep., 2011.
[11] **J. C. Peterson and M. B. Porter**, "Ray/beam tracing for modeling the effects of ocean and platform dynamics", *IEEE Journal of Oceanic Engineering*, vol. 38, no. 4, pp. 655–665, 2013.
[12] **C. Liu, Y. V. Zakharov, and T. Chen**, "Doubly selective underwater acoustic channel model for a moving transmitter/receiver", *IEEE Transactions on Vehicular Technology*, vol. 61, no. 3, pp. 938–950, 2012.
[13] **B. Henson, J. Li, Y. V. Zakharov, and C. Liu**, "Waymark Baseband Underwater Acoutic Propagation Model", In *IEEE Conference on Underwater Communications and Networking (UComms)*, Sestri Levante, Italy, pp. 1–5, 2014.
[14] **W. H. Tranter, T. S. Rappaport, K. L. Kosbar, and K. S. Shanmugan**, *Principles of communication systems simulation with wireless applications*, Prentice Hall New Jersey, vol. 1, 2004.
[15] **M. Stojanovic**, "Underwater acoustic communications: Design considerations on the physical layer", In *Fifth Annual IEEE Conference on Wireless on Demand Network Systems and Services*, Garmisch-Partenkirchen, Germany, pp. 1–10, 2008.
[16] **G. L. Stuber**, *Principles of mobile communication*, Springer Science & Business Media, 2011.
[17] **N. O. Booth, A. T. Abawi, P. W. Schey, and W. S. Hodgkiss**, "Detectability of low-level broad-band signals using adaptive matched-field processing with vertical aperture arrays", *IEEE Journal of Oceanic Engineering*, vol. 25, no. 3, pp. 296–313, 2000.
[18] **T. Chen, C. Liu, and Y. V. Zakharov**, Source localization using matched-phase matched-field processing with phase descent search", *IEEE Journal of Oceanic Engineering*, vol. 37, no. 2, pp. 261–270, 2012.